

F18-Fluorodeoxyglucose Positron Emission Tomography - Computed Tomography in Evaluation of Intracranial Space Occupying Lesions

Arshi Syed, Natasha Thakur, Syed Shafiq Alam, Syed Junaid
Department of Molecular Imaging, Fortis Hospital, Mohali, INDIA

Received: 22 August 2021 / Accepted: 11 April 2022 / Published online: 21 December 2022

OBJECTIVE: The aim of the study was to assess the diagnostic value of F-18 fluorodeoxyglucose (18F-FDG) positron emission tomography/computerized tomography (PET/CT) in evaluating and possible grading of intracranial space-occupying lesions.

METHODS: We included 27 patients from a tertiary care institute in north India. All patients were subjected to history taking, clinical examination, followed by baseline investigations and imaging. Cases were allocated to 4 distinct groups based on the World Health Organization (WHO) classification post-clinico-histological diagnosis: Low-grade tumors (25.9%), high-grade tumors (18.5%), metastases (48.1%), and other lesions (7.4%). Patients did contrast enhanced computerized tomography (CECT), contrast enhanced magnetic resonance imaging (CEMRI) and 18F-FDG PET/CT preoperatively. Postoperative follow-up was done, and the gold standard for tumor grading was the histopathology.

RESULTS: High-grade tumors (WHO Grade III/IV & IV/IV) did not show statistically significant standardized uptake values (SUV) max or SUVmax per unit volume indices compared with low-grade tumors or metastatic lesions.

CONCLUSION: The current study results suggests that 18F-FDG PET/CT indices of SUVmax or SUVmax per unit volume of the tumors by themselves are not reliable indices for differentiating high-grade tumors from lower grade ones or metastases; however, PET-CT imaging could rule out metastases from primary central nervous system (CNS) malignancies by evaluating the rest of the body.

KEYWORDS: Brain tumor, F-18 Fluorodeoxyglucose, Grading, Intracranial space-occupying lesions, Positron emission tomography/computerized tomography.

INTRODUCTION

Brain tumors are a common cause of cancer-related deaths in the middle-aged population, with an age-adjusted incidence of 28 per 100000 adults.¹ Metastasis is the most common cause of intracranial space-occupying lesions (ICSOL), followed by gliomas & meningiomas. Diagnosis of ICSOLs is generally based on clinical evaluation with neurological examination and anatomical imaging with CECT and CEMRI.^{1,2}

However, before the advent of anatomical imaging, molecular imaging and nuclear medicine had been at the leading research of brain function since the 1970s.¹ Technetium-99m (Tc-99m) radiopharmaceuticals scanning began in the 1960s with using pertechnetate and then was substituted by renal radiopharmaceuticals such as Technetium-99m glucoheptonate and Technetium-99m diethylene triamine pentaacetic acid (DTPA) that are devoid of the drawbacks of Tc-99m pertechnetate. Tc-99m glucoheptonate, Tc-99m tetrofosmin, Tc-99m sestamibi, & Thallium-201 distinguished brain tumors which involved multiple ways of uptake in addition to blood-brain barrier (BBB) disruption.³⁻⁶

Correspondence:

Syed Junaid
Department of Molecular Imaging, Fortis Hospital Mohali, india
Email: syedjunaidr@gmail.com

The development of radiotracer labelled metabolites like 18F-FDG and better multimodality imaging like PET/CT & PET/MRI have revolutionized brain lesions' early detection and characterization.⁷⁻²¹

Our work aimed to evaluate the semiquantitative estimation of uptake of 18F-FDG in tumor localization, characterization, grading and delineating brain tumors from non-neoplastic ring-enhancing lesions helping patient management.

PATIENTS AND METHODS

Twenty-seven patients were prospectively enrolled into the current study and radiographically evaluated after thorough clinical examination and brain tumor was suspected anatomically.

Acquisition and reconstruction parameters

A PET/CT scan was acquired 60 minutes after intravenous injection of approximately 180 – 370 mega becquerels (Bq) (5 - 10 milli Curie (mCi)) of 18F-FDG using a single bed position over 5 minutes. The raw data were reconstructed using ordered subset expectation maximization (OSEM), and CT attenuation correction was applied. The reconstructed data set was visualized in axial, sagittal and coronal slices and maximum intensity projections (MIP). After imaging, two trained specialists (in nuclear medicine and radiodiagnosis) evaluated the attenuation corrected PET/CT images. Metabolic tumor

volumes and 18F-FDG-standardized uptake values (corrected to lean body mass) were calculated in all the cases. The tumor SUV values (SUVmax & SUV average) were compared along the lines of tumor grading to find a correlation between them, which were then compared to visual grading of recent non-ionic CECT and/or gadolinium CEMRI of the same patients.

Patients were followed up for histopathological examination of the resected tumor, regarded as a gold standard for confirmation of tumor origin, histology and grading and outcome. Concurrently it was evaluated whether 18F-FDG scanning, in these cases, can be beneficial as a modality for brain tumor imaging or not. Similarly, the sensitivity and specificity of 18F-FDG were checked in detecting brain lesions. After acquiring all the data mentioned above, thorough statistical analyses were done to correct the difference between functional imaging with 18F-FDG PET/CT and anatomical imaging with modalities like CECT/ CEMRI on the same grounds.²²

Image analysis

The acquired 3D data was reconstructed into PET and CT slices on a multimodality workstation with the necessary imaging software. Software packages for current PET/CT systems allow visualization of PET, CT, and PET/CT fusion images in the axial, sagittal, coronal planes and the MIP in a 3D cine mode. The presence or absence of abnormal focal 18F-FDG accumulation in the PET images combined with their size and intensity was evaluated. In addition, criteria for visual analysis were defined for each study protocol. The SUV are increasingly used in clinical studies in addition to visual assessments and are a measurement of the uptake in a tumor normalized based on a distribution volume of interest (VOI).

Semiquantitative parameters were calculated as follows:

SUV = Activity per VOI x Act VOI (kBq/ml) ÷ Activity administered (MBq)/body weight (BW) (kg)

SUVmax determined uptake in the hottest pixel while SUVmean calculated the updated average over the entire volume of the lesion. These calculations measure activity in the regions of interest (ROI). Activity administered is the administered activity corrected for the physical decay of 18F-FDG to the start of acquisition. Patient height, weight was reported to allow for other SUV normalizations (lean body mass (LBM)).²¹

RESULTS

The image analysis and semiquantitative data analysis for 18F-FDG PET/CT, CECT and CEMRI are summarized in the master table. Patients were divided into four major groups.

Group 1: With WHO grade I/II tumors described in (Table 1) (n=7).

Group 2: With WHO grade III/IV tumors (n=5).

Group 3: With known cerebral metastases (n=13).

Group 4: With primary central nervous system (CNS) lymphoma (not classified in WHO classification) or tuberculoma (n=1).

Visual Analysis

a. Normal subjects

18F-FDG PET/CT, when performed on normal subjects, displayed a uniform, symmetrical uptake of the radiotracer predominantly in the cerebral gray matter and the basal ganglia with relatively lower uptake in the cerebral white matter. This demonstrates the exclusive metabolism of glucose in the brain tissues which is more in gray than white matter.²²

b. Positive subjects

Imaging was performed from 45 to 75 min post-injection of 18F-FDG using the standard imaging protocol. Lesions were described as those having uptake higher, equal to or lower than the surrounding brain tissues and than the baseline uptakes in the normal brain parenchyma in the contralateral hemisphere (using mirror ROIs).

Uptake of 18F-FDG was independent of the blood-brain barrier condition and was representative of tissue metabolism as the tracer is permeable to the intact blood-brain barrier.

High-grade tumors and primary CNS lymphomas (Fig. 1) showed relatively high uptake when compared to the surrounding brain tissues and mirror ROIs in the contralateral hemisphere; however, low-grade tumors / smaller lesions / necrotic lesions / some metastatic foci showed uptake equal to or lower than the adjacent gray matter (Fig. 2).

As most metastatic foci are usually present at the gray-white matter junction, some of these lesions could not be distinctly visualized in PET images even when they displayed mild enhancement on the CT component of the study (Fig. 3).

Although high-grade tumors usually showed higher SUVmax values than low-grade tumors, the difference was not estimated as statistically significant, thus proving that 18F-FDG PET/CT was generally equivocal in tumor grading in typical clinical scenarios.

Some non-malignant lesions like pituitary macroadenoma and tuberculoma (Fig. 4) displayed high SUVmax values, almost equivalent to those of high-grade tumors.

Follow-up of patients showed a statistically significant difference between the survival for low-grade tumors/ metastases from high-grade tumors.

Hence, it could be concluded that there was wide variation between tumor uptakes depending on tumor size, histology, tumor location, corticosteroid use, and infective lesions^{24,25}

Table 1: Comparison of CECT diagnosis with final diagnosis, HPE/Clinical (n=27)

	Hpe/Fd positive	Hpe/Fd negative	Total
CECT positive	22	1	23
CECT negative	4	0	4
	16	4	20

True Positive=22, True Negative=0, False Positive=1, False Negative=4
Sensitivity=84.6%, Positive Predictive Value=95.6%

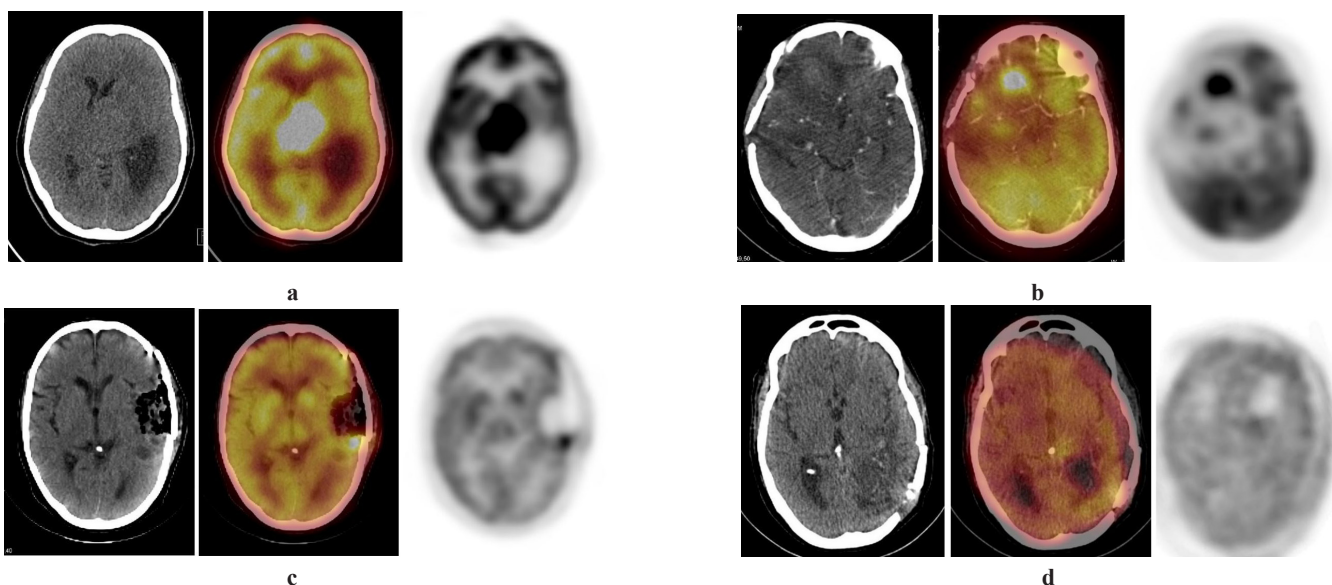


Fig 1: High grade gliomas (A) 18F-FDG PET/CT of a 42 years old female displayed a mass lesion in relation to the basal ganglia, histopathologically proven to be a high grade (WHO IV) glioma with a SUVmax of 13.0. **(B)** 18F-FDG PET/CT of a 53 years old female displayed a mass lesion in relation to the right frontotemporal region with associated perilesional edema, histopathologically proven to be a high grade (WHO III) glioma with a SUVmax of 7.5. **(C)** 18F-FDG PET/CT of a 59 years old male displayed a mass lesion in relation to the post-operative site in the left frontoparietal region with associated postsurgical gliotic changes, histopathologically proven to be recurrent high grade (WHO IV) glioma with a SUVmax of 4.8. **(D)** 18F-FDG PET/CT of a 56 years old male on steroids displayed a mass lesion in relation to the post-operative site in the left parieto-occipital region with associated postsurgical gliotic changes, histopathologically proven to be early recurrent high grade (WHO IV) glioma with a SUVmax of 2.5.

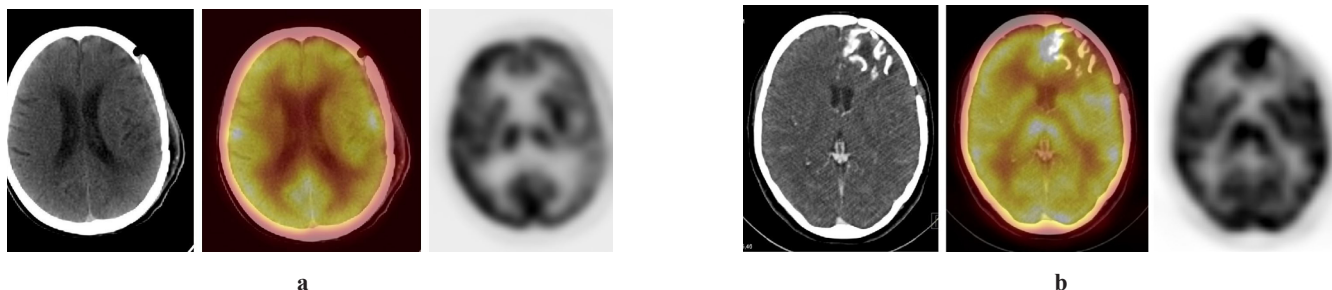


Fig 2: Low grade gliomas (A) 18F-FDG PET/CT of a 72 years old male displayed a non-enhancing non hypermetabolic mass lesion in relation to the left parietal region, histopathologically proven to be a low grade (II) astrocytoma with a SUVmax of 4.6. **(B)** 18F-FDG PET/CT of a 42 years old female displayed a mass lesion in relation to the left fronto-parietal region, histopathologically proven to be a low grade (II) oligodendroglioma with a SUVmax of 6.4.

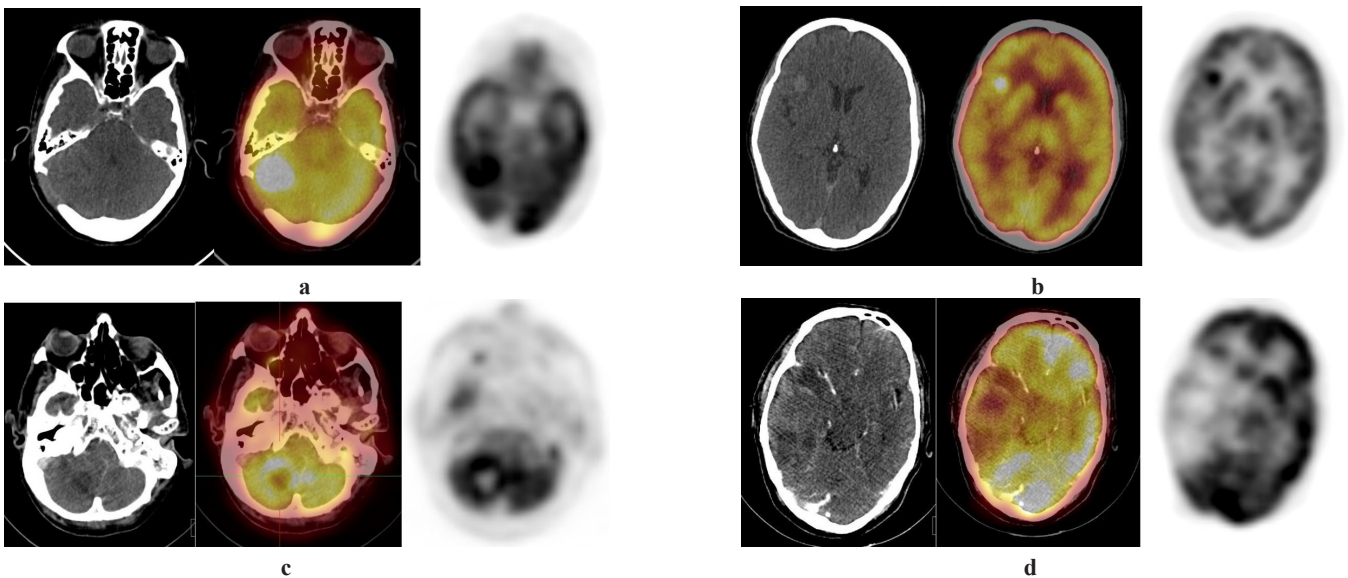


Fig 3: Metastases (A) 18F-FDG PET/CT of a 62 years old female displayed a mass lesion at the site of metastatectomy in relation to the right temporo-occipital region, histopathologically proven to be a recurrent metastasis with a SUVmax of 8.0. (B) 18F-FDG PET/CT of a 62 years old male displayed a mass lesion in relation to the right frontotemporal region, proven to be metastases from lung carcinoma with a SUVmax of 4.5. (C) 18F-FDG PET/CT of a 62 years old male displayed multiple mass lesion in the right frontoparietal region as well as right cerebellum, proven to be metastases from lung carcinoma with a SUVmax of 2.7. (D) 18F-FDG PET/CT of a 61 years old male displayed a mass lesion in relation to the right temporoparietal region with multiple areas of non-hypermetsabolic necrosis proven to be metastases from lung carcinoma with a SUVmax of 8.5.

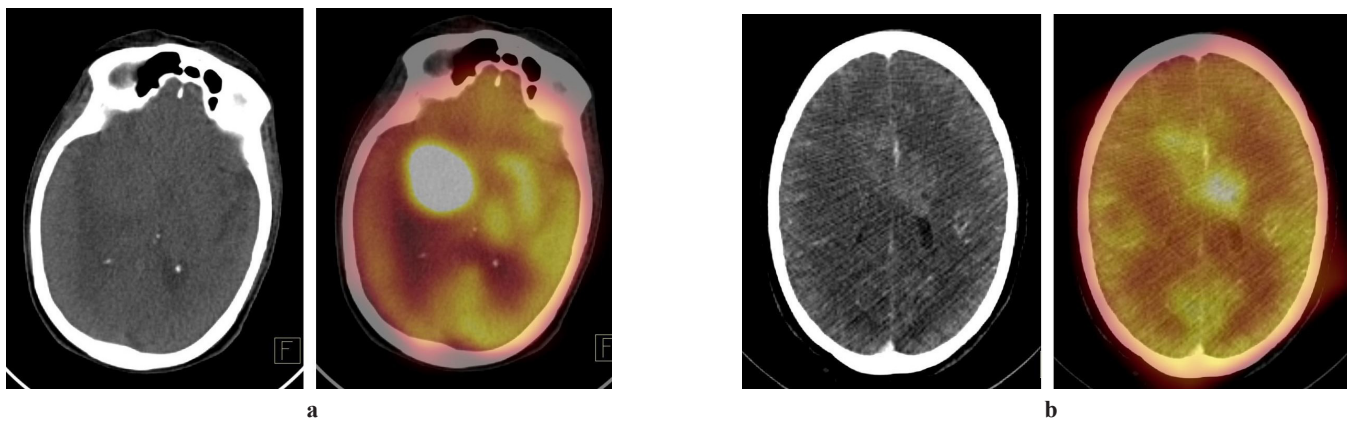


Fig 4: (A) 18F-FDG PET/CT of a 73 years old female displayed a mass lesion in relation to the right medial temporal lobe, histopathologically proven to be primary CNS lymphoma with a SUVmax of 16.8. (B) 18F-FDG PET/CT of a 60 years old female displayed few mass lesions in relation to the periventricular cortex diagnosed as tuberculoma with a SUVmax of 2.8.

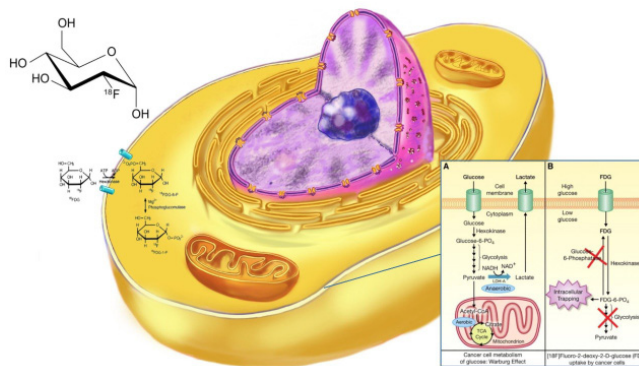


Illustration 1: The 18F-FDG molecule behaves similar to the glucose molecule and is transported into the cells via the glucose transporters (GLUT) receptors where it enters the glycolytic pathway and is acted upon by hexokinase to form FDG-6-phosphate. The subsequent enzyme (isomerase) is incapable of converting FDG-6-phosphate down the glycolytic pathway due to presence of a highly electronegative fluorine atom at the second carbon atom. In tumor cells which favor glycolysis over oxidative phosphorylation the GLUT receptors are upregulated, at the same time hexokinase activity is enhanced (Warburg’s effect) and glucose-6-phosphatase activity is diminished leading to trapping of the molecule preferentially within the tumor cells.

Anatomical imaging modalities

Contrast-enhanced computerized tomography

Evaluation of CECT is elaborated in (Table 2). Usually, small, low-grade tumors with an intact BBB were not detected as they did not show contrast enhancement. There was no clear-cut delineation between recurrent tumor and post-radiotherapy changes.

Contrast-enhanced magnetic resonance imaging

Evaluation of CEMRI is elaborated in (Table 2). The modality, however, could not exclusively distinguish between recurrent tumors or radiotherapy-induced gliosis.

Magnetic resonance spectroscopy (MRS) done in some of these subjects shows high choline to creatinine ratios (>2:1), suggesting active tumor growth, while those with significant necrosis displayed high lactate peaks; however, multi-voxel can be falsely positive in cases of demyelination. Histological diagnosis was available in all patients; 48.1% (n=13) showed cerebral metastases, 14.8% (n=4) showed glioblastoma multiforme, 18.2% (n=5) showed astrocytoma, 7.2% (n=2) showed oligodendroglioma, 3.7% (n=1) showed meningioma, 3.7% (n=1) showed primary CNS lymphoma and 3.7% (n=1) had tuberculoma.

Histopathological correlation

Cerebral metastases were the commonest histopathology, while astrocytoma was the commonest primary tumor, closely followed by glioblastoma multiforme.

Correlation between different imaging modalities.

Correlation of 18F-FDG PET/CT with CECT

Of the 27 patients evaluated with 18F-FDG PET/CT, all had undergone a contrast-enhanced computed tomography as the primary investigation.

Among these 27 patients, 18F-FDG PET/CT showed concordant results in 15 patients (55.5%), in 8 patients (29.6%) CECT was equivocal, while it was discordant in the remaining 4 patients (14.8%).

The CECT examinations were also performed as an adjunct of the PET/CT study acquired in tandem with PET (using Biograph 16, Siemens Corporation). Non-ionic contrast agents were used in all the patients to detect contrast-enhancing lesions and correlate with the BBB breakdown in the close vicinity of a malignant lesion.

If, for statistical purposes, the equivocal lesions were considered as positive concerning lesion detection as the doubt was concerning the pathological character of the lesion. The same can be visualized in (Table 2).

Correlation of 18F-FDG PET/CT with CEMRI

MRI is the gold standard for preoperative localization of ICSOLs. Gadolinium DTPA enhanced MRI was

performed in 100% (n=27) of patients. The results were concordant with ¹⁸F-FDG in 85.1% (n=23) of patients. However, it was discordant in one (low-grade oligodendroglioma, which could not be detected due to equal metabolism to the surrounding cerebral parenchyma and no contrast enhancement suggesting an intact BBB).

Three patients did MRS to delineate the chemical characteristics of the lesions. MRS results were concordant in one case and discordant in two. One was the correct final (clinico-histopathological) diagnosis. The same can be visualized in (Table 2).

The CEMRI examinations were performed on a 1.5T superconducting MRI (Avanto 1.5T, Siemens Corporation). Macrocyclic Gadolinium contrast enhancement was used in all studies. The statistical parameters of 18F-FDG PET/CT & CEMRI are described below:

Correlation of 18F-FDG PET/CT with final clinico-histopathological diagnosis

Twenty-two patients had pathological examination (group 2, 3, 4 patients and gliosis patients). Tumors were graded histopathologically using the WHO grading system.^{26,27}

Group 5 patients (n=4) were considered infarction/infection and managed accordingly with follow-up scans and improved during follow-ups as confirmed by the CECT/SPECT images. This suggested that the lesions are not of tumoural origin.

Correlation of 18F-FDG indices with histopathological grade (WHO classification)

Semiquantitative analysis was performed within all groups using the 18F-FDG metabolic indices, i.e. SUVmax and SUVmax/volume ratio. In addition, statistical evaluation was conducted to find a correlation between the tumor grade and his histopathological findings.

In most cases, the high-grade tumors did display higher SUVmax values and SUVmax/Volume ratios than the low-grade tumors; however, the results were not statistically significant (p=0.572).

Similarly, there was a significant overlap in the SUVmax values of high-grade tumors and metastatic lesions, and hence no cut-off values could be calculated by studying ROC characteristics that could differentiate low from high-grade tumors or metastases from high-grade tumors.

Analysis of variance (ANOVA) showed that although high grade (WHO Grade III and IV) tumors displayed higher SUVmax and SUVmax/volume ratio, there was no statistical difference within the groups.

Correlation of SUVmax with survival

18F-FDG PET SUV max showed insignificant power for predicting survival (p = 0.14). However, patients with high-grade gliomas usually survived for a shorter period

(median survival of 6 months) as compared to low-grade tumors (median survival of 9 months) and metastases (median survival of 18 months).

Kaplan–Meier survival curves demonstrated a significant power of histopathological grade and patient survival ($p = 0.001$).

There was a definite statistical difference between the histopathological grade and survival between the groups, with patients with metastatic brain lesions surviving for a significantly more extended time than high-grade and low-grade tumors.

Table 2: Anatomical Imaging Modality

Contrast-Enhanced Computed Tomography	
Negative	The Hounsfield unit density values are similar to the cerebrospinal fluid density
Positive (Tumor)	Effacement of the sulcal spaces adjacent to the lesion \pm contrast enhancement.
Contrast-Enhanced MRI	
Negative	No enhancement
Positive	<ul style="list-style-type: none"> ➤ They commonly showed contrast enhancement associated with necrosis, hemorrhage, mass effect, edema or signs of increased intracranial tension. ➤ Glioblastoma: Irregularly shaped foci (Necrosis) surrounded by ring enhancement.

DISCUSSION

Cancers lead to 9% of deaths worldwide and are the second cause of death in developed countries, next only to cardiovascular diseases.⁶ It comes as the 4th largest cause of mortality (6%) in less developed countries.⁶

CNS tumors were regarded earlier as relatively rare; however, with newer imaging modalities, it became clear that they accounted for 1.2% of autopsied deaths and 9% of cancers. Gliomas are central nervous system tumors derived from the glial cells representing the most common primary central nervous system tumors. While only about a quarter of intracranial tumors are due to gliomas, most deaths are due to glioma or intracranial space-occupying lesions. Despite being rare, adult gliomas have a marked public health effect.⁶

Advances in neurosurgical techniques, advanced radiotherapy planning (image-guided radiation therapy (IGRT), intensity-modulated radiation therapy (IMRT), gamma knife etc.), and cytotoxic and targeted chemotherapy for glial tumors treatment lead to an increased demand for non-invasive and accurate imaging techniques.

Regular MRI provides information on tumor volume and location and its characteristics such as mass effect, hemorrhagic, necrotic, surrounding edema, and increased intracranial pressure. Functional imaging adds complementary information, especially in post-treatment scenarios, differentiating residual/recurrent tumors from post-treatment gliotic changes and transforming tumors from low-grade to high-grade variants.^{9,14-16,25-51}

DTPA, Tc-99m GHA, Tc-99m, Thallium 201 have been successfully used in delineating or grading brain tumors on a gamma camera. The most significant disadvantage of these studies is the inherent lower scan sensitivity and resolution of single photon emission computerized tomography (SPECT) images.⁶

Imaging the brain using PET using 18F-FDG began in the 1970s at the Brookhaven National Laboratory and at the University of Pennsylvania, which resulted in the expansion of PET imaging. It was first administered at the University of Pennsylvania to two regular human volunteers by Alavi in 1976.^{26,28}

PET characterizes the tumor on a metabolic and molecular level and improves non-invasive tumor evaluation. This allows for customized treatment options and prognostication of the patient pre-and post-treatment. Depending on the radiotracer used, various molecular processes can be visualized, the vast majority of these agents being related to increased intratumoral cell proliferation.

This current study was designed to evaluate the use of 18F-FDG, the most widespread radiopharmaceutical currently used, given their applicability for diagnostic purposes and to provide an outlook for the future development of PET imaging with current scanners in gliomas.

Physiological brain glucose metabolism and 18F-FDG brain uptake are very high; thereby, 18F-FDG PET is a useful tool to image glial tumors because of the high correlation between malignancy and rate of glycolysis; therefore, there will be high rate of glucose metabolism in high grade tumors.³³ This was assumed to be associated with changes in rate of transport across glucose transporters (GLUTs); however one of the drawbacks of 18F-FDG PET is that its accuracy is hindered by increased metabolism of glucose in the brain, as previously discussed.^{16,27-29}

Decreased enhancement compared to the background can be rarely seen after management of high-grade gliomas, where uptake of 18F-FDG was less than or equal to the brain cortex. Although in some studies, uptake of 18F-FDG was correlated with tumor cellular density, glioma grade, and survival prognosis.^{14,16,22,30-43}

To differentiate between the slight contrast of glial tumors and normal gray matter, delayed (dual time point) scans between two to seven hours post-injection have been suggested, with few studies showing significant differences in SUVs of low-grade and high-grade tumors on delayed imaging. However, this might be challenging in a busy clinical setting.⁴⁴

Previously, radiolabeled amino acid PET is gaining popularity in diagnosing glial tumors as it addresses the drawbacks of 18F-FDG by showing better contrast between the tumor and background.^{37,39,45}

Newer tracers like C-11 methionine, F-18 Fluro methyl tyrosine, F-18 fluroethyl tyrosine, F-18 Fluro dopamine (DOPA) PET were shown to have certain benefits; however, the same were available at select centers and were economically not viable in smaller departments due to low yields.

The current study found that although the semiquantitative indices were higher in high-grade tumors than low-grade ones, there was no statistically significance to define a cut-off value even on the latest scanners in a typical clinical setting. However, it established that 18F-FDG PET/CT could yield complementary information when CEMRI alone was equivocal. It could also be used to rule out metastases (when used as part of a whole-body scan) and help in lesion characterization.

Future studies taking patient selection (pre-and post-treatment) and dual time point imaging will be sought to improve the results of FDG brain imaging, as has been determined by several study groups.^{41,48-51}

CONCLUSION

Our study reiterated some findings of the previous studies, which found 18F-FDG PET/CT helpful in delineating differences between different tumors; however, the semiquantitative indices performed at the typical 1-hour post-injection alone were not statistically significant to delineate low-grade tumors from high-grade ones in a typical clinical setting. The study, however, found that 18F-FDG PET could help in most cases to differentiate metastases based on concurrent whole-body imaging rather than tumor uptake indices.

Abbreviations

ANOVA: Analysis of variance.

BBB: Blood brain barrier.

Bq: Becquerels.

BW: Body weight.

CECT: Contrast enhanced computerized tomography.

CEMRI: Contrast enhanced magnetic resonance imaging.

Ci: Curie.

CNS: Central nervous system.

CT: Computerized tomography.

DOPA: Dopamine.

DTPA: Diethylene triamine pentaacetic acid.

FDG: Flurodeoxyglucose.

GLUT: Glucose transporter.

ICSOLs: Intracranial space occupying lesions.

IGRT: Image-guided radiation therapy.

IMRT: Intensity-modulated radiation therapy.

LBM: Lean body mass.

MIP: Maximum intensity projection.

MRI: Magnetic resonance imaging.

MRS: Magnetic resonance spectroscopy.

OSEM: Ordered subset expectation maximization.

PET: Positron emission tomography.

ROI: Region of interest.

SPECT: Single photon emission computerized tomography.

SUV: Standardized uptake values.

Tc-99m: Technetium-99m.

VOI: Volume of interest.

WHO: World Health Organization.

Disclosure

The authors report no conflict of interest in the materials or methods used in this study or the findings specified in this paper

Funding

The authors received no financial support for the research, authorship, and/or publication of this paper.

REFERENCES

1. Fishman RA. *Origins of neuroscience: A history of explorations into brain function*. First ed. New York: *Oxford University Press*. 1994.
2. Govindan R. *The Washington Manual of Oncology*. Second ed. St. Louis, Washington: *Lippincott Williams & Wilkins*. 2007.
3. Flitman SS. Survey of brain imaging techniques with implications for nanomedicine. Foresight Conference on Molecular Nanotechnology; 2000; *Bethesda, Maryland*.
4. Harvey A, Ziessman JPOM, James H, Thrall. *Nuclear Medicine: The Requisites*. Third ed: *Mosby*. 2006.
5. Peter J, Ell SG. *Nuclear Medicine in Clinical Diagnosis and Treatment*. Third ed. Philadelphia: *Churchill Livingstone*. 2004.
6. Alam SS, Junaid S, Ahmed SM. Evaluation of Technetium-99m glucoheptonate single photon emission computed tomography for brain tumor grading. *Asian J Neurosurg*. 2016;11(2):118-128.
7. Herholz K, Heiss WD. Positron emission tomography in clinical neurology. *Mol Imaging Biol*. 2004;6(4):239-269.
8. Patronas NJ, Di Chiro G, Brooks RA, et al. Work in progress: [18F] fluorodeoxyglucose and positron

- emission tomography in the evaluation of radiation necrosis of the brain. *Radiology*. 1982;144(4):885-889.
9. Ricci PE, Karis JP, Heiserman JE, Fram EK, Bice AN, Drayer BP. Differentiating recurrent tumor from radiation necrosis: time for re-evaluation of positron emission tomography? *AJNR Am J Neuroradiol*. 1998;19(3):407-413.
 10. Olivero WC, Dulebohn SC, Lister JR. The use of PET in evaluating patients with primary brain tumours: is it useful? *J Neurol Neurosurg Psychiatry*. 1995;58(2):250-252.
 11. Doyle WK, Budinger TF, Valk PE, Levin VA, Gutin PH. Differentiation of cerebral radiation necrosis from tumor recurrence by [18F]FDG and 82Rb positron emission tomography. *J Comput Assist Tomogr*. 1987;11(4):563-570.
 12. Wong TZ, van der Westhuizen GJ, Coleman RE. Positron emission tomography imaging of brain tumors. *Neuroimaging Clin N Am*. 2002;12(4):615-626.
 13. Weber MM. FDG normal brain scan and their anatomical features. *Am J Roentgenol Radium Ther Nucl Med*. 1965;94:815-818.
 14. Delbeke D, Meyerowitz C, Lapidus RL, et al. Optimal cutoff levels of F-18 fluorodeoxyglucose uptake in the differentiation of low-grade from high-grade brain tumors with PET. *Radiology*. 1995;195(1):47-52.
 15. Padma MV, Said S, Jacobs M, et al. Prediction of pathology and survival by FDG PET in gliomas. *J Neurooncol*. 2003;64(3):227-237.
 16. Di Chiro G, DeLaPaz RL, Brooks RA, et al. Glucose utilization of cerebral gliomas measured by [18F] fluorodeoxyglucose and positron emission tomography. *Neurology*. 1982;32(12):1323-1329.
 17. Borbely K, Fulham MJ, Brooks RA, Di Chiro G. PET-fluorodeoxyglucose of cranial and spinal neuromas. *J Nucl Med*. 1992;33(11):1931-1934.
 18. Griffith LK, Rich KM, Dehdashti F, et al. Brain metastases from non-central nervous system tumors: evaluation with PET. *Radiology*. 1993;186(1):37-44.
 19. De Souza B, Brunetti A, Fulham MJ, et al. Pituitary microadenomas: a PET study. *Radiology*. 1990;177(1):39-44.
 20. Heiss WD, Heindel W, Herholz K, et al. Positron emission tomography of fluorine-18-deoxyglucose and image-guided phosphorus-31 magnetic resonance spectroscopy in brain tumors. *J Nucl Med*. 1990;31(3):302-310.
 21. Kapoor V, McCook BM, Torok FS. An introduction to PET-CT imaging. *Radiographics*. 2004;24(2):523-543.
 22. Chen W. Clinical applications of PET in brain tumors. *J Nucl Med*. 2007;48(9):1468-1481.
 23. Kevin R. Carter EK. Common causes of false positive F18 FDG PET/CT scans in oncology. *Brazilian Archives of Biology and Technology*. 2007;50:29-35.
 24. Tripathi M, Jaimini A, D'Souza MM, et al. Spectrum of brain abnormalities detected on whole body F-18 FDG PET/CT in patients undergoing evaluation for non-CNS malignancies. *Indian J Nucl Med*. 2011;26(2):123-129.
 25. Gambhir SS. Molecular imaging of cancer with positron emission tomography. *Nat Rev Cancer*. 2002;2(9):683-693.
 26. Alavi A, Dann R, Chawluk J, Alavi J, Kushner M, Reivich M. Positron emission tomography imaging of regional cerebral glucose metabolism. *Semin Nucl Med*. 1986;16(1):2-34.
 27. Di Chiro G. Positron emission tomography using [18F] fluorodeoxyglucose in brain tumors. A powerful diagnostic and prognostic tool. *Invest Radiol*. 1987;22(5):360-371.
 28. Alavi JB, Alavi A, Chawluk J, et al. Positron emission tomography in patients with glioma. A predictor of prognosis. *Cancer*. 1988;62(6):1074-1078.
 29. Nagamatsu S, Sawa H, Wakizaka A, Hoshino T. Expression of facilitative glucose transporter isoforms in human brain tumors. *J Neurochem*. 1993;61(6):2048-2053.
 30. Weber W, Bartenstein P, Gross MW, et al. Fluorine-18-FDG PET and iodine-123-IMT SPECT in the evaluation of brain tumors. *J Nucl Med*. 1997;38(5):802-808.
 31. Schifter T, Hoffman JM, Hanson MW, et al. Serial FDG-PET studies in the prediction of survival in patients with primary brain tumors. *J Comput Assist Tomogr*. 1993;17(4):509-561.
 32. Chen W, Silverman DH, Delaloye S, et al. 18F-FDOPA PET imaging of brain tumors: comparison study with 18F-FDG PET and evaluation of diagnostic accuracy. *J Nucl Med*. 2006;47(6):904-911.
 33. Sasajima T, Miyagawa T, Oku T, Gelovani JG, Finn R, Blasberg R. Proliferation-dependent changes in amino acid transport and glucose metabolism in glioma cell lines. *Eur J Nucl Med Mol Imaging*. 2004;31(9):1244-1256.
 34. Cher LM, Murone C, Lawrentschuk N, et al. Correlation of hypoxic cell fraction and

- angiogenesis with glucose metabolic rate in gliomas using 18F-fluoromisonidazole, 18F-FDG PET, and immunohistochemical studies. *J Nucl Med.* 2006;47(3):410-418.
35. Herholz K, Pietrzyk U, Voges J, et al. Correlation of glucose consumption and tumor cell density in astrocytomas. A stereotactic PET study. *J Neurosurg.* 1993;79(6):853-858.
 36. Goldman S, Levivier M, Pirotte B, et al. Regional glucose metabolism and histopathology of gliomas. A study based on positron emission tomography-guided stereotactic biopsy. *Cancer.* 1996;78(5):1098-1106.
 37. Kaschten B, Stevenaert A, Sadzot B, et al. Preoperative evaluation of 54 gliomas by PET with fluorine-18-fluorodeoxyglucose and/or carbon-11-methionine. *J Nucl Med.* 1998;39(5):778-785.
 38. De Witte O, Levivier M, Violon P, et al. Prognostic value positron emission tomography with [18F] fluoro-2-deoxy-D-glucose in the low-grade glioma. *Neurosurgery.* 1996;39(3):470-476; discussion 476-477.
 39. Patronas NJ, Di Chiro G, Kufta C, et al. Prediction of survival in glioma patients by means of positron emission tomography. *J Neurosurg.* 1985;62(6):816-822.
 40. Pauleit D, Stoffels G, Bachofner A, et al. Comparison of (18)F-FET and (18)F-FDG PET in brain tumors. *Nucl Med Biol.* 2009;36(7):779-787.
 41. Spence AM, Muzi M, Mankoff DA, et al. 18F-FDG PET of gliomas at delayed intervals: improved distinction between tumor and normal gray matter. *J Nucl Med.* 2004;45(10):1653-1659.
 42. la Fougère C, Suchorska B, Bartenstein P, Kreth FW, Tonn JC. Molecular imaging of gliomas with PET: opportunities and limitations. *Neuro Oncol.* 2011;13(8):806-819.
 43. Kato T, Shinoda J, Nakayama N, et al. Metabolic assessment of gliomas using 11C-methionine, [18F] fluorodeoxyglucose, and 11C-choline positron-emission tomography. *AJNR Am J Neuroradiol.* 2008;29(6):1176-1182.
 44. Basu S, Alavi A. Partial volume correction of standardized uptake values and the dual time point in FDG-PET imaging: should these be routinely employed in assessing patients with cancer? *Eur J Nucl Med Mol Imaging.* 2007;34(10):1527-1529.
 45. Sasaki M, Kuwabara Y, Yoshida T, et al. A comparative study of thallium-201 SPET, carbon-11 methionine PET and fluorine-18 fluorodeoxyglucose PET for the differentiation of astrocytic tumours. *Eur J Nucl Med.* 1998;25(9):1261-1269.
 46. Povoski SP, Murrey DA, Jr., Smith SM, Martin EW, Jr., Hall NC. 18F-FDG PET/CT oncologic imaging at extended injection-to-scan acquisition time intervals derived from a single-institution 18F-FDG-directed surgery experience: feasibility and quantification of 18F-FDG accumulation within 18F-FDG-avid lesions and background tissues. *BMC Cancer.* 2014;14:453.
 47. De Witte O, Lefranc F, Levivier M, Salmon I, Brotchi J, Goldman S. FDG-PET as a prognostic factor in high-grade astrocytoma. *J Neurooncol.* 2000;49(2):157-163.
 48. Hustinx R, Smith RJ, Benard F, et al. Dual time point fluorine-18 fluorodeoxyglucose positron emission tomography: a potential method to differentiate malignancy from inflammation and normal tissue in the head and neck. *Eur J Nucl Med.* 1999;26(10):1345-1348.
 49. Zhuang H, Pourdehnad M, Lambright ES, et al. Dual time point 18F-FDG PET imaging for differentiating malignant from inflammatory processes. *J Nucl Med.* 2001;42(9):1412-1417.
 50. Kim DW, Jung SA, Kim CG, Park SA. The efficacy of dual time point F-18 FDG PET imaging for grading of brain tumors. *Clin Nucl Med.* 2010;35(6):400-403.
 51. Ghany AFA, Hamed MAG. The diagnostic value of dual phase FDG PET CT in grading of gliomas. *The Egyptian Journal of Radiology and Nuclear Medicine.* 2015;46(3):701-705.